

Microstructural and thermal property modifications of Sn-43Bi solder alloys via selective alloying with Se, In, Zn, and Al

Feryal Dawood¹, Abbas Al-Bawee², Ahmed A.A.G. Alrubaiy^{2*}

¹ College of Basic Education, University of Diyala, Baquba, Diyala, Iraq

² College of Engineering, University of Diyala, Baquba, Diyala, Iraq

* Corresponding author's e-mail: Ahmed_ail_eng@uodiyala.edu.iq

ABSTRACT

The impact of incorporating various alloying elements (Se, In, Zn and Al) into Sn43Bi solder alloys was investigated. These components fundamentally changed the microstructure and thermal properties of the base alloy. For instance, the particle size of Sn43Bi decreased from 465.58 Å to 217.09 Å with the addition of 2 wt% In. With Sn43Bi2In showing the lowest contact angle of 21.5°, compared to 23.34° for the base alloy, the contact angle, a gauge of wettability improved especially. With the addition of 2 wt% In, thermal analysis showed that the melting temperature of Sn43Bi dropped from 139 °C to 114 °C, the pasty range closed from 10.4 °C to 7.5 °C. On the other hand, Al raised the pasty range and the melting temperature. These results show that particular alloying elements can maximize the mechanical and thermal characteristics of Sn-Bi solder alloys, so improving their suitability for electronic uses.

Keywords: matrix structure, melting temperature, thermal properties, pasty range, contact angle, tin-bismuth alloy.

INTRODUCTION

The purpose of the study was to explore the effect of including several alloying elements (such selenium, indium, zinc and aluminum) into tin-bismuth-based solder alloys. This work focused on variations in the matrix structure, thermal properties and melting temperature, pasty range, contact angle (wettability) of the Sn43Bi alloy following element insertion. By systematically examining these effects, the authors aimed to determine the best composition that enhances the performance of lead free solder alloys, which makes them suitable for technology applications while dealing with environmental and safety concerns associated with common lead-based solders. Se, In, Zn and Al were chosen as alloying elements based on their known effects on improving the properties of Sn-Bi alloys. For example, In has been shown to lower the melting point and enhance mechanical properties. The 2 wt% concentration was selected based on preliminary experiments and literature reviews. High-purity metals (99.9% or above), especially

chosen for their potential to form effective lead-free solder alloys constituted the foundation elements for the conducted research. Algailani et al. (1) highlighted the growing industrial adoption of environmentally friendly technologies supporting the authors' argument for continued development of lead-free solder alternatives. This study is particularly relevant, as the semiconductor industry continues to evolve its materials in response to environmental and health concerns. For connecting electronic circuit components, tin-lead alloys are the most often used ones. Along with many advantages including rather good welding, manufacturability, high dependability, and low cost (2), these alloys enable the welding process conditions compatible with most materials. However, despite these great features that have been demonstrated in various studies, the presence of lead, a hazardous element, affects the surrounding environment (3). The semiconductor industry is transitioning away from lead containing solder alloys due to concerns about lead toxicity and its environmental and health

impacts prompting the European Union's Restriction of Hazardous Substances (RoHS) directive to control and reduce lead consumption in electrical and electronic devices (4).

Studies have found that specific alloying elements can greatly affect the mechanical and thermal properties of Sn-Bi alloys. Ag/Cu has been shown for instance, to enhance mechanical strength and enthalpy change (ΔH) during phase transitions (5). Meanwhile, Ga/In lowers melting points, increases specific heat capacity (C_p), enhances thermal conductivity (6). Other elements like Sb/Zn stabilize microstructures and reduce thermal expansion (6,7). Additionally, Mn/Si/Fe balance between fluidity, oxidation resistance, and thermal conductivity (8). Collectively, these modifications optimize Sn-Bi alloys for low-temperature soldering, thermal reliability, and energy-efficient applications (5, 9).

Nevertheless, attaining comparable performance to traditional Pb-based solders poses substantial technical hurdles. Recent studies have highlighted the importance of understanding the electromigration behavior of Sn-Bi solders, which is significantly influenced by alloying elements (10,11). Indium (In) has been shown to greatly reduce the melting point, and change the microstructure when added to different solder alloys, including Sn-0.7Cu and 42Sn-Bi, so rendering them fit for low-temperature uses (12). Thus, it is imperative to maximize alloy compositions to raise the performance of solders free of lead. Given this imperative, Sn-Bi alloys, known for their low melting temperatures, can be further optimized with alloying elements like Se and Zn (13). Beyond microstructural adjustments, thermal and mechanical reliability also require optimization. Sn-Bi alloys exhibit specific heat capacities consistent with theoretical predictions (7). In turn, Ga additions further enhance thermal energy storage capabilities (6).

This is achieved by adjusting the internal structure and relieving the stress that triggers whisker growth (14). The study highlights the necessity of reducing tin concentrations in solder alloys to reduce health risks. Rising awareness of lead toxicity has increased the demand for lead-free solder alternatives and stimulated substantial research within the electronics industry to develop effective and environmentally sustainable soldering solutions. Making lead-free solder alloys is quite challenging, especially when trying to replace traditional lead-containing materials with

desired mechanical and thermal properties. One study by El-Taher et al. (15) for instance looks at how the switch to lead-free solders has spurred research of new alloy compositions to either match or exceed the performance of conventional lead-containing solders. Major challenges include:

Melting point: Lead free solders generally exhibit higher melting points than lead based solders, complicating manufacturing processes and increasing energy consumption (15).

Mechanical properties: Studies have shown that adding Sb and Ag to Sn-Bi alloys refines the microstructure, reduces the size of the bismuth-rich phase, and enhances mechanical properties (16–18). Research shows that varying Bi concentrations in Sn-xBi-1Ag solders and adding Si affects such properties as Cu_6Sn_5 layer thickness, tensile strength, microhardness, melting temperature, and wettability (19).

Increasing Bi content reduces oxidation resistance but extends the melting range and increases the spreading rate. Bi's control of IMC generation lowers IMC thickness even above 3 wt.% Bi. Indium addition improves the naturally brittle SnBi alloy by increasing mechanical properties and reducing brittleness. For instance, In enhances mechanical strength and the enthalpy change (ΔH) during phase transitions (20). Studies show that small amounts of Ni and carbon fiber can enhance ductility and fracture toughness in Sn58Bi solder joints (21). The resulting Sn-Bi-In alloy demonstrates enhanced wettability and refined microstructural properties (22).

Likewise, it has been demonstrated that adding indium (In) and silicon (Si) to Sn-Bi solder alloys improves mechanical properties including tensile strength and refines microstructures and changes thermal properties including melting temperature (23). Although some components, such as In and Si, enhance specific characteristics, a study by Dirasutisna et al. (24) showed that adding aluminum (Al) to Sn-52Bi raised the melting point so highlighting the influence of Al in changing thermal behavior. Using their low melting temperatures, substrate compatibility and fit for thermal interface materials, research on seven Sn-Bi alloys also showed their potential as lead-free solder substitutes (25). To solve important issues in their development, the microstructure and thermal properties of Sn-Bi solder alloys are greatly influenced by the addition of alloying elements, including selenium, indium, zinc and aluminum. These results stress the need of balancing

mechanical and thermal characteristics for best solder performance. Mn lowers thermal conductivity in Sn-Bi-Sb alloys, while In/Si increase it and Si/Fe increase fluidity without sacrificing conductivity (26). Beyond mechanical characteristics, solder performance is greatly influenced by thermal stability:

Thermal fatigue – lead-free solders are more prone to thermal fatigue than lead-based solders because of their different thermal expansion coefficients, which over time increases the risk of cracking and failure in electronic components (27).

Wettability and solder joint reliability – lead-free solders often have poorer wettability, which hinders the formation of reliable solder joints by affecting the ability of the solder to bond effectively to surfaces. Optimizing alloy composition is essential to improve wettability and joint reliability (14).

Researchers have used alloying elements to enhance solder performance and address these challenges. The incorporation of alloying elements such as selenium (Se), indium (In), zinc (Zn), and aluminum (Al) into Sn-Bi solder alloys has a substantial impact on their microstructure and thermal characteristics (28). Indium (In) has been extensively studied for its ability to enhance the properties of Sn-Bi solder alloys. For example, adding 1.5 wt% In to Sn-58Bi modifies the microstructure, improves impact toughness (20), as well as enhanced thermal and mechanical properties (29). Li et al. (30) noted the role of In in improving ductility and reducing brittleness in Sn-Bi-In low-temperature solders.

X-ray diffraction studies showed these additions changed phase composition. For instance, it has been demonstrated that adding a small amount of Al to Sn-based eutectic alloys improves the microstructure and hence increases solder joint strength by changing intermetallic phase development (11). Another study (30) underlined enhanced thermal and mechanical characteristics of indium additions to Sn-Bi solders. Increasing indium content changed the microstructure and distribution of Sn and Bi phases.

This study investigates how certain alloying elements (Se, In, Zn, Al) modify the microstructure and thermal properties of Sn43Bi alloys. By understanding these modifications, the findings contribute to the development of solder materials with improved wettability, lower melting temperatures, and reduced tin content, addressing both cost-effectiveness and environmental compliance.

MATERIALS AND METHODS

The environmental concern has driven the electronics industry to seek sustainable alternatives that maintain performance while eliminating toxic elements necessitates limiting its use in the electronic field (31). From this perspective, it was vital to look for more environmentally friendly solder alloys that are non-toxic and devoid of hazardous lead. According to the Restriction of Hazardous Substances (RoHS) directive for electrical and electronic waste it was essential to develop non-toxic, lead-free solder alternatives.

Lead-free tin-based systems have shown promise for being environmentally friendly substitutes based on preliminary tests of novel substances (4). High-purity metals (99.9% or above) especially chosen for their potential to form effective lead-free solder alloys constituted the foundation elements for this research. These metals include tin, bismuth, zinc, indium, and aluminum. After precise weighing and mixing according to predetermined compositions, the alloys were melted and cast under controlled atmospheric conditions (temperature: 25 °C, pressure: 1 atm, humidity: 40%) to ensure consistent quality. The alloys made of tin and bismuth are ready for all the tests. For structural characterization, an X-ray diffractometer (Shimadzu DX-30, Japan) was employed using Cu-K α radiation at 45 kV and 35 mA, equipped with nickel filters, and operated over an angular range of 2 θ from 0° to 100° in continuous mode with a scan speed of 5°/min. SEM analysis was performed using a 20 kV, 10 mm SEM providing a depth of field 300 times greater than optical microscopes and microstructural characterization was performed using a JEOL JSM-6510 LV. Thermographs were produced by differential scanning calorimetry (DSC) with a heating rate of 10 °C/min across a temperature range of 0 °C to 300 °C, thus enabling exact analysis of thermal properties such as phase transition temperatures, enthalpy/entropy change values at phase transitions, etc. Nawi et al. (32) showed that the thermal conditions during processing significantly affect material properties. This emphasizes the importance of controlled thermal processing conditions in analyzing solder, alloys as temperature variations can significantly influence their microstructure and performance.

RESULTS AND DISCUSSION

X-ray diffraction

X-ray diffraction patterns of Sn₄₃Bi₂X (X = Se or In or Zn or Al) alloys have lines corresponding to β-Sn, Bi and SnBi intermetallic phases as shown in Figures 1 to Figure 5. The addition of Zn, Al and In elements altered the lattice parameters and unit cell volume of the Sn phase leading to changes in the XRD patterns. For example, the addition of In refined the microstructure and reduced particle size, thereby shifting the diffraction peak positions. The analysis of X-ray shows that, adding different alloying elements (Se or In or Zn or Al) to Sn₄₃Bi alloy caused a change in formed matrix structure (started base line, peak intensity, peak broadness and position). This is due to the presence of dissolved Se, In, Zn, or Al atoms in the alloy matrix, resulting in a solid solution. Other

accumulating elements may also create undiscovered phases. The details of formed phases (2θ, intensity, d Å, full width at half maximum, phases and Miller indices) of Sn₄₃Bi₂X alloys are listed in Table 1. Lattice parameters (a and c), unit cell volume (V) and particle size (ε) of tetragonal tin phase for Sn₄₃Bi₂X alloys are presented in Table 2. The outcomes reveal that the parameters of the lattice and unit cell volume values for Sn₄₃Bi alloy changed after adding Se, In, Zn, or Al, although the particle size value declined.

Scanning electron microscope analysis

Scanning electron micrographs (SEM) of Sn-43B-2X (X = Se, In, Zn and Al) alloys are shown in Figure 6. SEM analysis of the Sn₄₃Bi alloy, Figure 6, showed different Sn grains with different sizes and orientations. Microstructure of

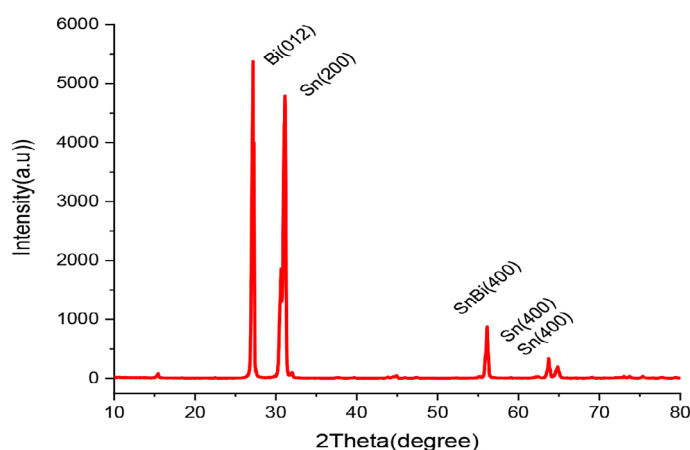


Figure 1. X-ray diffraction patterns of Sn-43Bi alloy, measured at 25 °C

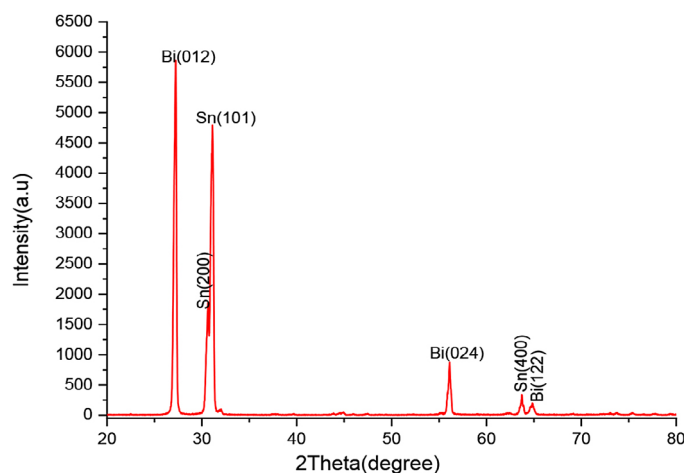


Figure 2. X-ray diffraction patterns of Sn-43Bi-2Se alloy, measured at 25°

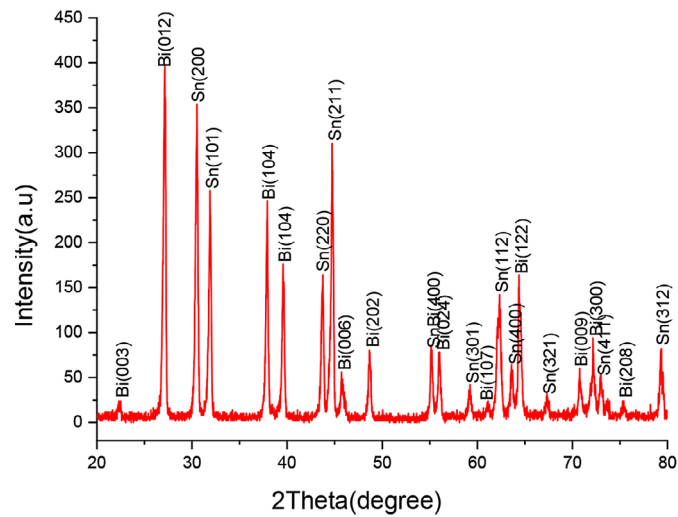


Figure 3. X-ray diffraction patterns of Sn-43Bi-2In alloy, measured at 25 °C

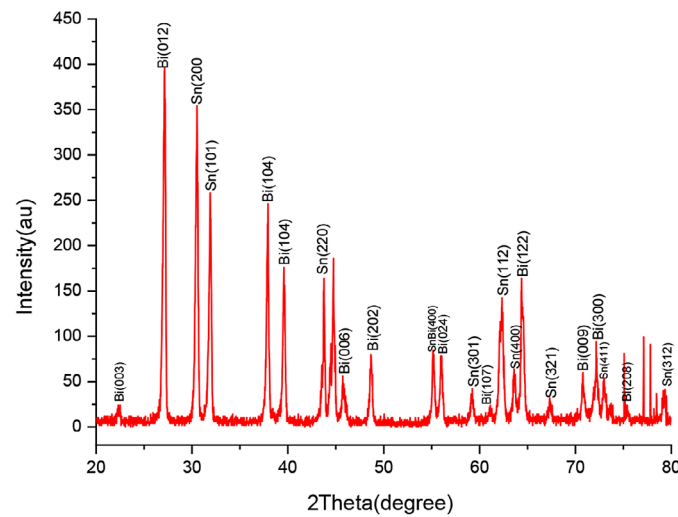


Figure 4. X-ray diffraction patterns of Sn-43Bi-2Zn alloy, measured

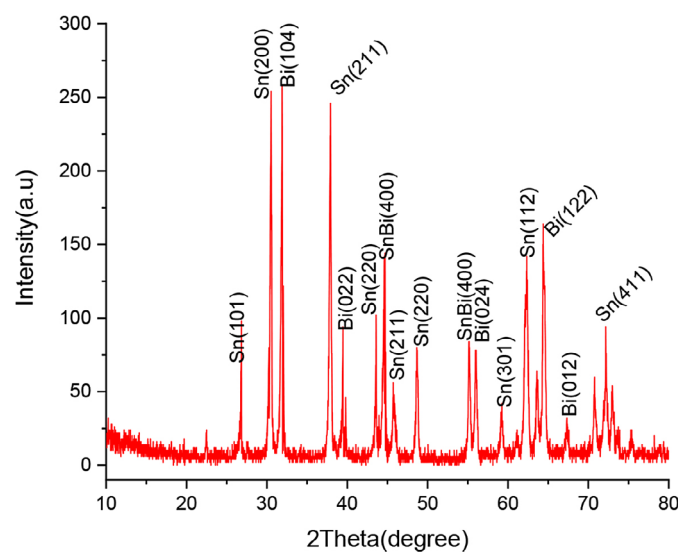


Figure 5. X-ray diffraction patterns of Sn-43Bi-2Al alloy, measured at 25 °C.

Sn43B2X alloy such as Sn grains (size and orientations) and other formed phases (Bi and SnBi, and Si) with little variation on matrix alloy after adding 2 wt% from (X = Se, In, Zn, and Al) content, as seen in Figure 6. Similar to the obtained findings, Al-Katawy et al. (33) demonstrated that the addition of bismuth and gallium significantly refined the microstructure of low alloy steel, thus enhancing its mechanical properties. This refinement in microstructure correlates with improved mechanical properties, as evidenced by the changes in grain size and phase distribution observed in the conducted study. It aligns with

authors' finding that adding particular alloying elements to Sn43Bi solder alloys can improve their mechanical properties. Mohamed et al. (34) demonstrated that adding alumina nanomaterials to the products can significantly improve mechanical performance. This is further supported by the SEM analysis in Figure 6 which displays finely tuned microstructures that enhance mechanical properties. This meant that, in line with the development of non-symmetry phases with different chemical compositions, size and orientations exhibited a significant heterogeneity of microstructure which will relate to the X-ray analysis.

Table 1. X-ray diffraction analysis of Sn43Bi alloy, including 2θ, d spacing, full width at half maximum (FWHM), intensity, phase (indicating the crystal structure of the compound), and Miller indices

| Alloys | 2θ ±0.1 | d Å ±0.01 | FWHM (Å) ±0.05 | Intensity Counts ±3 | Phase | hkl |
|-------------|---------|-----------|----------------|---------------------|-------|-----|
| Sn-43Bi | 27.32 | 3.26 | 0.31 | 35 | Bi | 012 |
| | 30.72 | 2.90 | 0.19 | 35 | Sn | 200 |
| | 55.24 | 1.66 | 0.17 | 6 | SnBi | 400 |
| | 63.74 | 1.45 | 0.18 | 7 | Sn | 400 |
| | 64.39 | 1.20 | 0.17 | 13 | Sn | 312 |
| Sn-43Bi-2Se | 27.20 | 3.27 | 0.32470 | 100 | Bi | 012 |
| | 30.64 | 2.92 | 0.39800 | 30 | Sn | 200 |
| | 31.08 | 2.87 | 0.36990 | 82 | Sn | 101 |
| | 56.09 | 1.63 | 0.29160 | 15 | Sn | 024 |
| | 63.72 | 1.46 | 0.2600 | 6 | Sn | 301 |
| Sn-43Bi-2In | 27.21 | 3.27 | 0.63 | 59 | Bi | 012 |
| | 30.68 | 2.91 | 0.71 | 94 | Sn | 200 |
| | 32.16 | 2.78 | 0.56 | 100 | Bi | 104 |
| | 36.60 | 2.45 | 0.41 | 84 | Sn | 211 |
| | 38.04 | 2.36 | 0.57 | 43 | Bi | 022 |
| | 39.75 | 2.26 | 0.56 | 39 | Sn | 220 |
| | 44.93 | 2.01 | 0.54 | 59 | Sn | 211 |
| | 46.03 | 1.97 | 0.480 | 13 | Bi | 006 |
| | 48.85 | 1.86 | 0.51 | 23 | Bi | 202 |
| | 55.40 | 1.65 | 0.44 | 18 | SnBi | 400 |
| | 56.15 | 1.63 | 0.42 | 30 | Bi | 024 |
| | 59.47 | 1.55 | 0.46 | 8 | Sn | 301 |
| | 62.43 | 1.48 | 0.59 | 30 | Sn | 112 |
| | 63.81 | 1.45 | 0.37 | 19 | Sn | 301 |
| | 64.68 | 1.43 | 0.39 | 48 | Bi | 122 |
| | 67.55 | 1.38 | 0.42 | 6 | Sn | 321 |
| | 70.95 | 1.32 | 0.42 | 14 | Bi | 009 |
| | 72.00 | 1.31 | 0.42 | 8 | Bi | 300 |
| | 72.40 | 1.30 | 0.24 | 13 | Sn | 420 |
| | 73.19 | 1.29 | 0.46 | 17 | Sn | 420 |
| 75.49 | 1.25 | 0.32 | 6 | Sn | 312 | |
| 79.54 | 1.20 | 0.36 | 26 | Sn | 330 | |

| | | | | | | |
|-------------|--------|------|------|-----|------|-----|
| Sn-43Bi-2Zn | 27.07 | 3.29 | 0.21 | 53 | Bi | 012 |
| | 30.46 | 2.93 | 0.21 | 100 | Sn | 200 |
| | 31.82 | 2.80 | 0.22 | 29 | Sn | 101 |
| | 37.81 | 2.37 | 0.19 | 12 | Bi | 104 |
| | 39.51 | 2.27 | 0.21 | 12 | Bi | 100 |
| | 43.61 | 2.07 | 0.19 | 32 | Sn | 220 |
| | 44.64 | 2.02 | 0.20 | 27 | Sn | 211 |
| | 48.52 | 1.87 | 0.21 | 6 | Bi | 202 |
| | 55.07 | 1.66 | 0.16 | 13 | SnBi | 400 |
| | 55.91 | 1.64 | 0.19 | 13 | SnBi | 400 |
| | 61.98 | 1.49 | 0.10 | 6 | Bi | 107 |
| | 62.22 | 1.49 | 0.25 | 12 | Sn | 112 |
| | 63.50 | 1.46 | 0.18 | 14 | Sn | 321 |
| | 64.32 | 1.40 | 0.23 | 17 | Bi | 122 |
| | 72.08 | 1.31 | 0.17 | 26 | Sn | 420 |
| | 72.84 | 1.29 | 0.18 | 9 | Sn | 411 |
| 79.17 | 1.21 | 0.18 | 11 | Sn | 312 | |
| Sn-43Bi-2Al | 27.124 | 3.28 | 0.30 | 102 | Bi | 012 |
| | 30.52 | 2.92 | 0.29 | 87 | Sn | 200 |
| | 31.93 | 2.81 | 0.27 | 100 | Sn | 101 |
| | 37.89 | 2.37 | 0.24 | 58 | Bi | 104 |
| | 39.58 | 2.27 | 0.26 | 42 | Sn | 220 |
| | 44.35 | 2.03 | 0.17 | 11 | Sn | 211 |
| | 44.74 | 2.02 | 0.25 | 77 | Bi | 006 |
| | 45.77 | 1.98 | 0.26 | 11 | Sn | 211 |
| | 48.67 | 1.86 | 0.20 | 20 | Sn | 220 |
| | 55.16 | 1.66 | 0.26 | 23 | SnBi | 400 |
| | 55.99 | 1.64 | 0.21 | 21 | Bi | 024 |
| | 59.18 | 1.55 | 0.25 | 9 | Sn | 301 |
| | 62.43 | 1.48 | 0.29 | 31 | Sn | 112 |
| | 63.60 | 1.46 | 0.21 | 15 | Sn | 400 |
| | 64.41 | 1.44 | 0.16 | 44 | Bi | 122 |
| | 67.32 | 1.38 | 0.26 | 6 | Bi | 122 |
| | 70.76 | 1.33 | 0.24 | 13 | Bi | 009 |
| | 71.92 | 1.31 | 0.23 | 8 | Bi | 300 |
| 72.19 | 1.31 | 0.22 | 18 | Sn | 420 | |
| 72.98 | 1.29 | 0.22 | 11 | Sn | 411 | |

Thermal properties

The comprehensive data in Table 3 provides valuable insights into how different alloying elements can be used to tailor the thermal performance of Sn-Bi solder alloys for specific electronic packaging applications, balancing requirements for thermal management, and electrical performance. With indium and selenium raising density while zinc somewhat lowering it, the density values ranging from 7.3 to 7.9 g/cm³ reflect

the atomic masses of the added element. The thermal modification effects observed in the conducted study align with the findings of Elmnifi et al. (35) they showed that controlled thermal processing can significantly alter material properties for specific applications.

Different alloying elements affect the unique trends in the thermal characteristics of the Sn-Bi alloys. Reflecting the well-known effect of indium in reducing the eutectic point and aluminum in raising it, the melting temperature shows notable

Table 2. Lattice parameters, unit cell volume and particle size of Sn-43Bi-2X alloys, measured at 25 °C

| Alloys | a (Å) ± 0.005 | c (Å) ± 0.005 | V (Å ³) ± 0.1 | ε (Å) ± 2.0 |
|--------------------------|---------------|---------------|---------------------------|-------------|
| Sn-43Bi | 5.822 | 3.334 | 113.01 | 465.58 |
| Sn-43Bi-2Se | 5.831 | 3.387 | 115.12 | 274.571 |
| Sn-43Bi-2In | 5.823 | 3.382 | 114.67 | 217.090 |
| Sn-43Bi-2Zn ₂ | 5.864 | 3.359 | 115.49 | 420.076 |
| Sn-43Bi-2Al | 5.855 | 3.168 | 108.6 | 387.310 |

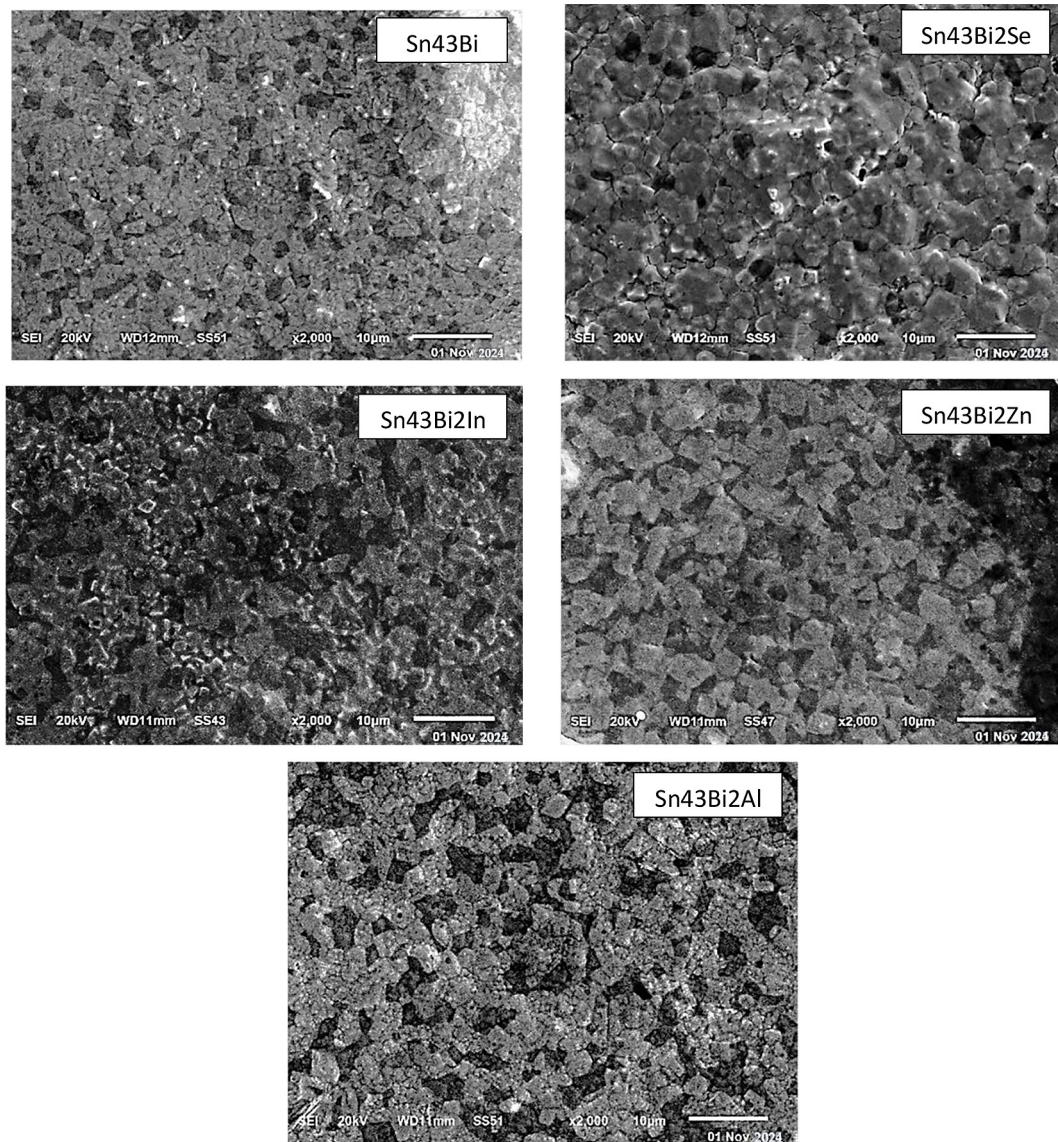


Figure 6. SEM micrographs of Sn-43Bi-2X (X = Se, In, Zn, and Al) alloys at 2000x magnification, measured at 25 °C

variation ranging from 114 °C for Sn-43Bi-2In to 154 °C for Sn-43Bi-2Al. Typical for metallic solders the specific heat capacity stays rather constant among the alloys ranging from 0.20 to 0.23 J/g·K. With ranges of 1.10–1.35 mm²/s thermal diffusivity shows how alloying elements

affect heat propagation across a material. Thermal diffusivity ($\alpha = k/(\rho \cdot C_p)$) is indirectly affected by alloying. For instance, in the additions that increase (k) and reduce (ρ), (α) may enhance, while elements like Mn (lowering k) or Ga (increasing C_p) could reduce α (6, 26).

Table 3. Thermal properties of Sn-43Bi-2X alloys, including thermal conductivity, specific heat capacity, thermal diffusivity, and electrical conductivity, measured using differential scanning calorimetry and electrical conductivity tests

| Alloy | ΔH (J/g) ± 1 | C_p (J/g·K) ± 0.02 | k (W/m·K) ± 1 | α (mm ² /s) ± 0.05 | σ , $\times 10^7$ (ohm ⁻¹ ·cm ⁻¹) ± 0.02 |
|-------------|--------------------------|--------------------------|---------------------|--|--|
| Sn-43Bi | 50 | 0.22 | 22 | 1.35 | 4.5 |
| Sn-43Bi-2Se | 48 | 0.20 | 18 | 1.20 | 3.0 |
| Sn-43Bi-2In | 52 | 0.23 | 24 | 1.32 | 5.0 |
| Sn-43Bi-2Zn | 49 | 0.21 | 20 | 1.30 | 4.0 |
| Sn-43Bi-2Al | 47 | 0.20 | 17 | 1.10 | 3.5 |

The thermal conductivity values show interesting fluctuations where Sn-43Bi-2In exhibits the highest thermal conductivity (24 W/m·K) presumably because of the special microstructural effects of indium, the other alloys show lower conductivity than the base Sn-43Bi. Similar to the obtained findings, Mahan et al. (36) demonstrated that adding mineral significantly enhances thermal insulation properties, highlighting the potential of composite materials in thermal management applications. This aligns with the drawn observation that specific alloying elements can modify the thermal conductivity of Sn-Bi solder alloys, as seen in Table 3. The electrical conductivity values display a clear relationship with the alloying elements, ranging from $3.0\text{--}5.0 \times 10^7 \text{ ohm}^{-1}\cdot\text{cm}^{-1}$, with Sn-43Bi-2In showing the highest conductivity. This suggests that indium addition maintains better electronic structure for conduction despite its microstructural effects on thermal properties.

Soldering properties

Wettability is measured quantitatively using the contact angle produced at the flux triple point of the solder substrate. Thermal analysis is frequently used to investigate solid state changes as well as solid-liquid interactions. Pasty range is the difference between solidus and liquidus values. Figure 7 depicts the DSC thermographs of SnBi43(2X), (X = Se, In, Zn, or Al) alloys. These figures determine the melting point and pasty

range of the employed alloys. The DSC analysis revealed variations in melting points and pasty ranges, Al raised the values while Se, In and Zn lowered them. The DSC measurements were repeated multiple times to ensure reliability and the results shown in Figure 7 are representative and consistent across all measurement cycles. For example, adding 2 weight percent reduced the melting temperature of Sn43Bi from 139 °C to 114 °C and closed the pasty range from 10.4 °C to 7.5 °C. Alloying elements affect the enthalpy of fusion (ΔH). For Sn-Ag-Cu (SAC) alloys, for instance, the hypoeutectic SAC037 solder displays a ΔH of 64.4 J/g (37). Ag or Cu can form intermetallic compounds (e.g., Ag-Sn, Cu-Sn) with enthalpies of formation ranging from -86 to 25 kJ/mol in Sn-Bi systems, thus influencing the total thermal behavior (5).

The contact angles for Sn-43Bi-2X, (X= Se or In or Zn or Al) alloys on Cu substrate in air are listed in Table 4. The contact angle of Sn₅₇Bi₄₃ alloy varied after adding alloying elements. Melting temperature and pasty range for Sn₄₃Bi alloy decreased after adding Se, In, Zn but they increased after adding Al.

Contact angle (wettability)

Wettability is quantitatively assessed by the contact angle formed at the flux triple point of the solder substrate. The contact angles of Sn-43Bi (Se, In, Zn, or Al) melt spun alloys on Cu

Table 4. Contact angle, melting temperature and pasty range for Sn-43Bi-2X alloys, with error values indicated

| Alloys | Contact angle θ (°) $\pm 1^\circ$ | Melting temperature (°C) ± 2 | Pasty range (°C) ± 0.5 |
|-------------|--|----------------------------------|----------------------------|
| Sn-43Bi | 23.34 | 139 | 10.4 |
| Sn-43Bi-2Se | 33.14 | 127 | 14.1 |
| Sn-43Bi-2In | 21.5 | 114 | 7.5 |
| Sn-43Bi-2Zn | 28.25 | 129 | 9.4 |
| Sn-43Bi-2Al | 43.11 | 154 | 15 |

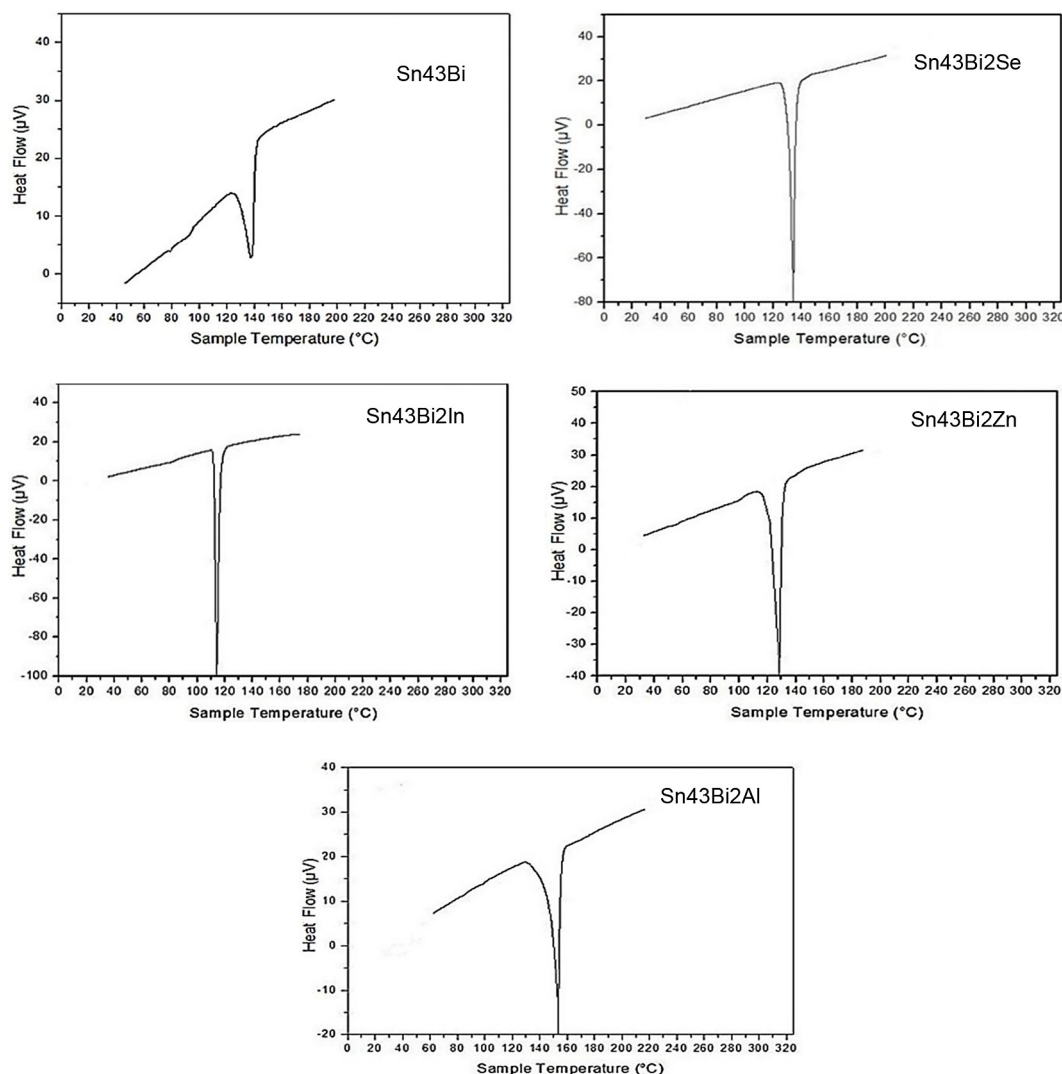


Figure 7. DSC thermographs of Sn-43Bi-2X (X = Se, In, Zn, or Al) alloys. The displayed temperature ranges were selected to highlight the key thermal events (melting and pasty ranges) relevant to the performance of solder alloys in typical electronic applications

Table 5. Contact angle of Sn-43Bi melt spun alloys on Cu substrate

| Alloy | Contact angle (Θ_0) \pm 0.5° |
|-------------|---|
| Sn-43Bi | 42.59 |
| Sn-43Bi-2Se | 55.52 |
| Sn-43Bi-2In | 32.57 |
| Sn-43Bi-2Zn | 39.29 |
| Sn-43Bi-2Al | 43.11° |

substrates are shown in Table 5. From these results, it is clear that adding Bi content to Sn43Bi melt-spun alloy caused a significant effect in contact angle value and wettability, of it. Shehab et al. (38) noted that surface treatment, and alloy composition significantly affect wettability in welding processes similar to how the investigated alloying

elements influenced contact angles in soldering applications. The Sn76Zn9Bi15 melt spun alloy has a lower contact angle and good wetting on copper substrate.

CONCLUSIONS

The microstructure and thermal characteristics of Sn43Bi solder alloys are significantly altered by the addition of Se, In, Zn and Al. These elements modify the lattice parameters and unit cell volume of the tin phase, influencing particle size and phase generation. For example, adding two weight percent of various elements changed the particle size of Sn43Bi from 465.58 to 217.09 Å. Especially Sn-43Bi-2In showed the

lowest contact angle of 21.5° , indicating higher wettability than the base alloy. The DSC analysis highlighted that Al increased melting points and pasty ranges, while Se, In, and Zn had the opposite effect. Specifically, adding 2 weight percent In reduced the melting temperature of Sn-43Bi from 139°C to 114°C and narrowed the pasty range from 10.4°C to 7.5°C . These results taken together confirm that Sn-Bi solder alloys mechanical and thermal characteristics can be maximized by carefully selecting alloying elements for electronic uses. Future studies should investigate the combined effects of several alloying elements to improve these characteristics even more.

REFERENCES

- Algailani HM, Al-Nassar SI, Mahmoud AK, Ali AA. Synthesis of bio-nanocomposite coating (silver-multi wall carbon nano tubes) by electroless plating method. *Materials Today: Proceedings*. 2023; <https://doi.org/10.1016/j.matpr.2023.02.017>
- de Carvalho CC, Sobral BS, de Sousa RB, Paixão JL, de Araújo Dantas SL, Spinelli JE, et al. Effects of different zinc content on solidification, microstructure, and mechanical properties in tin–bismuth alloy. *Advanced Engineering Materials*. 2024;26(21): 2401074
- Hmadeh L, Jaculli MA, Vedvik N, Elahifar B, Sangesland S. The effect of temperature on the sealability of bismuth–tin alloy plugs. *Geoenergy Science and Engineering*. 2024;241: 213107.
- SunderRaj AJ, Ananthapadmanaban D. Environmental aspects of lead free soldering and study of legislations banning lead based solders in different countries. *Environmental Science*. 2024;3(1): 87.
- Flandorfer H, Saeed U, Luef C, Sabbar A, Ipser H. Interfaces in lead-free solder alloys: Enthalpy of formation of binary Ag–Sn, Cu–Sn and Ni–Sn intermetallic compounds. *Thermochimica Acta*. 2007;459(1–2): 34–39. <https://doi.org/10.1016/j.tca.2007.04.004>
- Wang Q, Cheng X, Li Y, Yu G, Liu Z. Microstructures and thermal properties of Sn–Bi–Zn–Ga alloys as heat transfer and heat storage materials. *Journal of Wuhan University of Technology-Mater. Sci. Ed.* 2019;34(3): 676–683. <https://doi.org/10.1007/s11595-019-2103-1>
- Bozinovic K, Manasijevic D, Balanovic L, Gorgievski M, Stamenkovic U, Markovic M, et al. Study of microstructure, hardness and thermal properties of Sn-Bi alloys. *Hemijaska industrija*. 2021;75(4): 227–239. <https://doi.org/10.2298/HEMIND210119021B>
- Hou W, Wang J, Li H. Theoretical investigation of thermodynamic properties of the Al–Si–Fe ternary alloy. *ACS Omega*. 2024;9(6): 6316–6324. <https://doi.org/10.1021/acsomega.3c03921>
- Hao Q, Tan XF, Gu Q, Sweatman K, McDonald SD, Nogita K. The Effects of temperature and solute diffusion on volume change in Sn-Bi solder alloys. *JOM*. 2022;74(4): 1739–1750. <https://doi.org/10.1007/s11837-021-05145-4>
- Ali HE, El-Taher AM, Algarni H. Influence of bismuth addition on the physical and mechanical properties of low silver/lead-free Sn-Ag-Cu solder. *Materials Today Communications*. 2024;39: 109113. <https://doi.org/10.1016/j.mtcomm.2024.109113>
- Singh P, Palmer L, Wassick T, Aspandiar R, Franco B, Swaminathan LA, et al. Recent iNEMI research on electromigration in Tin-Bismuth solder. In: 2024 IEEE 40th International Electronics Manufacturing Technology (IEMT). IEEE; 2024; 1–7. <https://doi.org/10.1109/IEMT61324.2024.10875254>
- Lv X, Pan Z, Liu Y, Zhang C, Wang Z, Sun F. Effects of Bi and In addition on microstructure and properties of Sn-0.7Cu solder. *Metals*. 2025;15(2): 157. <https://doi.org/10.3390/met15020157>
- Luktuke A, Kastengren AL, Nikitin V, Torbati-Sarraf H, Chawla N. Bismuth pyramid formation during solidification of eutectic tin-bismuth alloy using 4D X-ray microtomography. *Communications Materials*. 2024;5(1): 95.
- Xu KK, Zhang L, Gao LL, Jiang N, Zhang L, Zhong SJ. Review of microstructure and properties of low temperature lead-free solder in electronic packaging. *Science and Technology of Advanced Materials*. 2020;21(1): 689–711.
- El-Taher AM, Ali HE, Algarni H. Enhancing performance of Sn–Ag–Cu alloy through germanium additions: Investigating microstructure, thermal characteristics, and mechanical properties. *Materials Today Communications*. 2024;38: 108315.
- Peng YZ, Li CJ, Yang JJ, Zhang JT, Peng JB, Zhou GJ, et al. Effects of bismuth on the microstructure, properties, and interfacial reaction layers of Sn-9Zn-xBi solders. *Metals*. 2021;11(4): 538.
- Wu Y, Fowler HN, Weddington N, Blendell JE, Handwerker CA. Effect of Sb and Ag additions on the melting and solidification of Sn-Bi solder alloys. *MRS Advances*. 2023;9(1): 2–6. <https://doi.org/10.1557/s43580-023-00619-w>
- Yan J, Xiao W, Wang J, Zhang F, Li X, He H, et al. Effects of alloying elements on the interfacial segregation of bismuth in tin-based solders. *Materials Today Communications*. 2023;35: 105713. <https://doi.org/10.1016/j.mtcomm.2023.105713>
- Chen S, Wang X, Guo Z, Wu C, Liu Y, Liu Y, et al. Investigation of the microstructure, thermal properties, and mechanical properties of Sn-Bi-Ag

- and Sn-Bi-Ag-Si low temperature lead-free solder alloys. *Coatings*. 2023;13(2): 285. <https://doi.org/10.3390/coatings13020285>
20. Zhang H, Zhang Q, Song Z. Influences of low In alloying and aging on microstructure and plastic deformation behavior of Sn-58Bi solder. *Journal of Materials Science: Materials in Electronics*. 2024;35(17): 1185.
 21. Kong X, Liu Z, Ma R, Zhai J, Pan Z, Li X, et al. Microstructural and mechanical responses of Sn-58Bi/Cu composite solder joints with 0.1 wt.% Ni and carbon fiber addition. *Scientific Reports*. 2024;14(1): 32141.
 22. Liu Y, Tu KN. Low melting point solders based on Sn, Bi, and In elements. *Materials Today Advances*. 2020;8: 100115. <https://doi.org/10.1016/j.mtadv.2020.100115>
 23. Kang H, Rajendran SH, Jung JP. Low melting temperature Sn-Bi solder: Effect of alloying and nanoparticle addition on the microstructural, thermal, interfacial bonding, and mechanical characteristics. *Metals*. 2021;11(2): 364. <https://doi.org/10.3390/met11020364>
 24. Dirasutisna DT, Soegiono B, Kurniawan B, Masduki MY. Analysis of thermal properties of solder material Sn-Bi-Al using differential scanning calorimetry (DSC). *J. Adv. Res. Mater. Sci*. 2016;18: 1–9.
 25. Bozinovic K, Manasijevic D, Balanovic L, Gorgjevski M, Stamenkovic U, Markovic M, et al. Study of microstructure, hardness and thermal properties of Sn-Bi alloys. *Hemijaska industrija*. 2021;75(4): 227–239. <https://doi.org/10.2298/HEMIND210119021B>
 26. Mosaad S, Mohamed AR, Kamal M. Characterization of Indium addition on Sn-Bi-Sb lead free solder alloy. *Journal of advances in physics*. 2016;12(2).
 27. Depiver JA. Thermo-mechanical reliability studies of lead-free solder interconnects. University of Derby (United Kingdom); 2021.
 28. Tao Y, Xue S, Liu H, Long W, Wang B. Effect of Cr addition on microstructure and properties of AuGa solder. *Metals*. 2020;10(11): 1449.
 29. Chen X, Xue F, Zhou J, Yao Y. Effect of In on microstructure, thermodynamic characteristic and mechanical properties of Sn-Bi based lead-free solder. *Journal of Alloys and Compounds*. 2015;633: 377–383. <https://doi.org/10.1016/j.jallcom.2015.01.219>
 30. Li Q, Lei Y, Lin J, Yang S. Design and properties of Sn-Bi-In low-temperature solders. In: 2015 16th International Conference on Electronic Packaging Technology (ICEPT). IEEE; 2015; 497–500. <https://doi.org/10.1109/ICEPT.2015.7236635>
 31. Anuar NEE, Singh A, Mei Kit ML, Choo HL, Durairaj R, Janasekaran S. Investigation on the thermal and wettability properties aided with mechanical test simulation of tin (Sn)-bismuth (Bi) solder alloy at low reflow temperatures. *Key Engineering Materials*. 2024;982: 99–114.
 32. Nawi SA, Mohammed HB, Jasim AN, Sharaf HK, Muhammad MT. Numerical analysis of the influence of the rolling speed on the cold rolling under specific thermal condition of the AA 5052-O aluminum alloy. *Journal of Advanced Research in Fluid Mechanics and Thermal Sciences*. 2024;122(1): 69–79. <https://doi.org/10.37934/arfmts.122.1.6979>
 33. Al Katawy AA, Alrubaiy AAAG, Jomah AJS. Enhancing mechanical properties of low alloy steel through novel molten Bi-Ga austempering. *Diyala Journal of Engineering Sciences*. 2024;17(2): 173–181. <https://doi.org/10.24237/djes.2024.17212>
 34. Mohamed MT, Nawi SA, Algailani HM, Alrubaiy AAAG, Mahmoud AK, Farman S, et al. Evaluation of the mechanical performance of iron- polymethyl methacrylate and polystyrene polymer products based on alumina nanomaterials. *Advances in Science and Technology Research Journal*. 2025;19(3): 202–210. <https://doi.org/10.12913/22998624/199471>
 35. Elmnifi M, Mansur AN, Abdul-Ghafoor QJ, Alrubaiy AAAG, Mustafa MAS, Khaleel M, et al. Induction heating for residential water desalination: A numerical simulation and experimental evaluation. *International Journal of Heat and Technology*. 2023;41(6): 1433–1440. <https://doi.org/10.18280/ijht.410605>
 36. Mahan HM, Katawy A, Shabeeb OA, Alrubaiy AAAG. Analyzing thermal insulation of concrete polymer by adding mineral wool. *Advances in Science and Technology Research Journal*. 2025;19(5): 430–439. <https://doi.org/10.12913/22998624/202766>
 37. Drienovsky M, Palcut M, Priputen P, Cuninková E, Bošák O, Kubliha M, et al. Properties of Sn-Ag-Cu solder joints prepared by induction heating. *Advances in Materials Science and Engineering*. 2020;2020(1). <https://doi.org/10.1155/2020/1724095>
 38. Shehab AA, Nawi SA, Al-Rubaiy AA, Hammoudi Z, Hafedh SA, Abass MH, et al. CO₂ laser spot welding of thin sheets AISI 321 austenitic stainless steel. *Archives of Materials Science and Engineering*. 2020;2(106): 68–77. <https://doi.org/10.5604/01.3001.0014.6974>